Contact parameter estimation using a constrained extended Kalman filter

L. Mazzanti [1,2], **M. Vivet** [1,2], **D. De Gregoriis** [1, 2], **T. Tamarozzi** [2], **B. Blockmans** [2, 3]
[1] Siemens Digital Industries Software,
Interleuvenlaan 68 B-3001, Leuven, Belgium
e-mail: **lorenzo.mazzanti@siemens.com**

[2] KU Leuven, Department of Mechanical Engineering,
Celestijnenlaan 300, B-3001, Heverlee, Belgium

[3] DMMS Core lab, Flanders Make, Belgium

Abstract
In structural dynamics simulations, sophisticated contact models are required to accurately describe contact interactions. These contact models typically depend on several, possibly uncertain, parameters. In recent years, significant efforts have been spent in developing hybrid techniques that enhance the predictive performance of numerical models with real-world measured data. The Virtual Sensing (VS) estimation framework uses a Kalman Filter-based approach to combine experimental measurement data with numerical models. In this work, an extension of VS for contact model parameter estimation is presented. The developed VS formulation is numerically validated using a lumped-parameter model of a mass-spring-damper system to demonstrate the potential of the methodology. The objective of the experiment is accurate joint state-contact parameter estimation, starting from an inaccurate system model. Results show that the inclusion of contact parameter in the estimation improves the accuracy of the overall estimation.

1 Introduction

Nonlinear, non-smooth systems are present in multiple engineering applications. Simulation models capable of accurately capturing this behaviour often require the usage of formulations characterized by multiple parameters. Important non-smooth phenomena in the field of mechanics across many industrial contexts are contact interactions. Modelling these interactions and the corresponding computational mechanics aspects have been studied extensively [1], but accurate contact simulation typically still requires prior knowledge or an estimate of multiple parameters used by so-called contact models. Uncertainty on the values of these quantities may influence the overall accuracy of simulation results. The accurate estimation of these contact model parameters is therefore of great importance, but this task is often challenging, especially when dealing with strongly nonlinear, non-smooth systems.

In recent years, hybrid deterministic-stochastic state estimation techniques based on the Augmented Kalman filter have been successfully used for structural mechanics applications, especially for input estimation [2, 3, 4, 5]. Many extensions of the canonical Kalman filter formulation have been proposed throughout the years to handle nonlinear systems [6]. Equality and inequality constraints can also be integrated into the estimation process [7]. In [8] an Augmented Extended Kalman filter approach for parametric estimation on non-smooth systems is proposed. In [9], the authors propose an Augmented Extended Kalman filter for parameter estimation that preserves estimator stability when a subset of states become non-observable.

Within the concept of Virtual Sensing, a state estimator, typically an (Augmented) Kalman filter, is used to retrieve quantities that are difficult to directly measure by means of estimating the system states, inputs and parameters and using these to extract the quantities of interest. Figure 1 shows a schematic representation

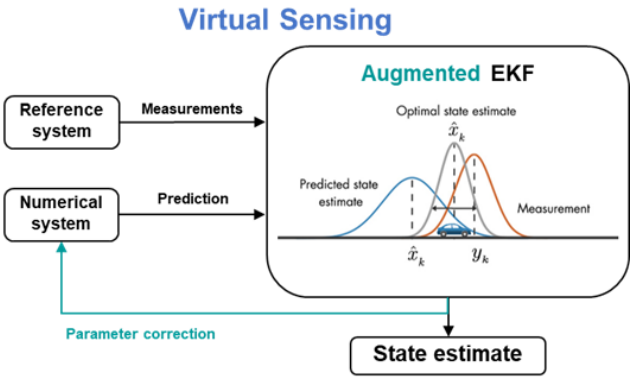

Figure 1: A schematic representation of the concept of Virtual Sensing for parameter estimation. The estimator corrects states and (user-defined) parameters of the system's numerical model to obtain an accurate estimate of difficult to measure quantities.

of the concept. This work aims at extending existing Kalman filter-based methods to create such a Virtual Sensing application capable of correctly estimating contact model parameters, handling the intrinsic non-smoothness and nonlinearity of the contact phenomena and its effects on the definition of a stable estimation algorithm.

2 The augmented extended Kalman filter

The theoretical background needed for the Virtual Sensing for contact parameters framework is provided in this section. The estimator of choice for this application is the Augmented Extended Kalman filter (AEKF) [6]. For the purpose of introducing the AEKF, it is assumed that the considered dynamic system is described using the following implicit state-space continuous time formulation, whereas the proposed estimation framework is based on the method proposed in [4]:

$$\mathbf{g}(\dot{\mathbf{x}}, \mathbf{x}, \mathbf{u}, \mathbf{p}) = \mathbf{0} \tag{1}$$

Here, $\mathbf{x} \in \mathbb{R}^{n_s}$ is the state vector, $\mathbf{u} \in \mathbb{R}^{n_u}$ is the input vector, $\mathbf{p} \in \mathbb{R}^{n_p}$ is the parameter vector. Furthermore, n_s is the number of system states, n_u is the number of inputs, n_p is the number of parameters.

This work focuses on parameter estimation using an AEKF. The state vector is therefore augmented to include the parameters of interest as additional states to be estimated. Here, these parameters are represented using the parameter vector $\mathbf{p}$ introduced above:

$$\mathbf{x}^* = \begin{bmatrix} \mathbf{x} \\ \mathbf{p} \end{bmatrix} \tag{2}$$

Where $\mathbf{x}^* \in \mathbb{R}^{n_s+n_p}$ is the resulting augmented state vector. As a consequence, the state-space formulation used in the AEKF requires a model that describes the time evolution of $\mathbf{p}$. In this work, a zero-th order random walk model is adopted [10]. The augmented state space formulation $\mathbf{g}^*$ then becomes:

$$\mathbf{g}^*(\dot{\mathbf{x}}^*, \mathbf{x}^*, \mathbf{u}) = \begin{bmatrix} \mathbf{g}(\mathbf{x}, \mathbf{u}, \mathbf{p}) \\ \dot{\mathbf{p}} \end{bmatrix} = \mathbf{0} \tag{3}$$

Where

$$\dot{\mathbf{x}}^* = \begin{bmatrix} \dot{\mathbf{x}} \\ \dot{\mathbf{p}} \end{bmatrix} \tag{4}$$

Additionally, the so-called measurement equation is defined as:

$$\mathbf{y} = \mathbf{h}(\mathbf{x}^*) \tag{5}$$

Where $\mathbf{y} \in \mathbb{R}^{n_o}$ is the measurement (output) vector and $\mathbf{h} \in \mathbb{R}^{n_o}$ is, in general, a nonlinear function. Furthermore, n_o is the number of outputs that are provided to the AEKF to perform the estimation.

In this work, a discrete time AEKF is used to perform state-parameter estimation. The implicit formulation $\mathbf{g}^*(\dot{\mathbf{x}}^*, \mathbf{x}^*, \mathbf{u})$ is time-discretized using a backward Euler scheme.

The corresponding discrete-time state-space formulation for Eq. (3) is defined as:

$$\mathbf{g_d}(\mathbf{x}_k^*, \mathbf{x}_{k-1}^*, \mathbf{u}_k) = \mathbf{0} \tag{6}$$

Where k refers to the discrete time $t_k = k\Delta t$, where Δt is the timestep size.

A stochastic component is introduced to describe uncertainties on both the system dynamics and the measurement equation. The full discrete-time state-space formulation, including the measurement equation, then becomes:

$$\begin{cases} \mathbf{g_d}(\mathbf{x}_k^*, \mathbf{x}_{k-1}^*, \mathbf{u}_k) - \omega_\mathbf{k} = \mathbf{0} \\ \mathbf{y}_k = \mathbf{h}(\mathbf{x}_k^*) + \epsilon_k \end{cases} \tag{7}$$

Here, ω_k and ϵ_k represent the process and measurement noise, respectively. They are assumed to be white, zero mean, uncorrelated random processes with known (diagonal) covariance matrices $\mathbf{Q}_k$ and $\mathbf{R}_k$, respectively. The structure of $\mathbf{Q}_k$ is therefore:

$$\mathbf{Q}_k = \begin{bmatrix} \mathbf{Q}_{\mathbf{x},k} & \mathbf{0} \\ \mathbf{0} & \mathbf{Q}_{\mathbf{p},k} \end{bmatrix} \tag{8}$$

The estimator provides an estimate of the first two statistical moments of $\mathbf{x}^*$ given the sequence of measurements $\{\mathbf{y_k}\}$ and inputs $\{\mathbf{u_k}\}$. The first moment is the mean value of the estimate, referred to as $\hat{\mathbf{x}}^*$, the second moment is the state error covariance matrix $\mathbf{P}$, defined using the expected value operator $\mathbb{E}$ as:

$$\mathbf{P} = \mathbb{E}[(\mathbf{x}^* - \hat{\mathbf{x}}^*)(\mathbf{x}^* - \hat{\mathbf{x}}^*)^T] \tag{9}$$

An estimation timestep consists of a prediction step, in which the evolution of the estimate is predicted and the error covariance matrix is propagated using the state-space model (Eq. (7)), and a correction step, in which the estimate is corrected as to match the provided measurement data.

The superscript $\square^-$ refers to estimates or function evaluations corresponding to a post-prediction step estimate. The superscript $\square^+$ instead refers to estimates or function evaluations corresponding to a post-correction step estimate. Throughout the estimation process, linearization of the discrete-time functions $\mathbf{g_d}$ and $\mathbf{h}$ is required. The linearized matrices $\mathbf{F}_k, \mathbf{H}_k$ are defined as:

$$\mathbf{F}_k = -\left(\frac{\partial \mathbf{g_d^*}}{\partial \mathbf{x}^*}\Big|_{\mathbf{x}_k^* = \hat{\mathbf{x}}_k^{*-}}\right)^{-1} \frac{\partial \mathbf{g_d^*}}{\partial \mathbf{x}^*}\Big|_{\mathbf{x}_k^* = \hat{\mathbf{x}}_{k-1}^{*+}} \tag{10}$$

$$\mathbf{H}_k = \frac{\partial \mathbf{h}}{\partial \mathbf{x}_k^*}\Big|_{\mathbf{x}_k^* = \hat{\mathbf{x}}_k^{*-}} \tag{11}$$

The matrix $\mathbf{F}_k$ is used to propagate $\mathbf{P}_k$ during the prediction step:

$$\mathbf{P}_k^- = \mathbf{F}_k \mathbf{P}_{k-1}^+ \mathbf{F}_k^T + \mathbf{Q}_k \tag{12}$$

The matrix $\mathbf{H}_k$ is required to compute the Kalman Gain matrix $\mathbf{G}_k \in \mathbb{R}^{(n_s+n_p)\times n_o}$, which is used to perform the correction of $\hat{\mathbf{x}}_k, \mathbf{P}_k$.

$$\mathbf{G}_k = \mathbf{P}_k^- \mathbf{H}_k^T (\mathbf{H}_k \mathbf{P}_k^- \mathbf{H}_k^T + \mathbf{R}_k)^{-1} \tag{13}$$
$$\hat{\mathbf{x}}_k^{*+} = \hat{\mathbf{x}}_k^{*-} + \mathbf{G}_k(\mathbf{y}_k - \mathbf{H}\hat{\mathbf{x}}_k^{*-}) \tag{14}$$
$$\mathbf{P}_k^+ = (\mathbf{I} - \mathbf{G}_k \mathbf{H}_k)\mathbf{P}_k^- \tag{15}$$

An overview of the estimation process at each timestep k is presented in Table 1.

Table 1: Overview of the AEKF estimation process steps.

AEKF estimation process
Prediction step:
$\mathbf{g_d}(\hat{\mathbf{x}}_k^{*-}, \hat{\mathbf{x}}_{k-1}^{*+}, \mathbf{u}_k) = \mathbf{0}$
$\mathbf{F}_k = -\left(\frac{\partial \mathbf{g_d^*}}{\partial \mathbf{x}^*}\Big\|_{\mathbf{x^*}_k=\hat{\mathbf{x}}_k^{*-}}\right)^{-1} \frac{\partial \mathbf{g_d^*}}{\partial \mathbf{x}^*}\Big\|_{\mathbf{x^*}_k=\hat{\mathbf{x}}_{k-1}^{*+}}$
$\mathbf{P}_k^- = \mathbf{F}_k \mathbf{P}_{k-1}^+ \mathbf{F}_k^T + \mathbf{Q}_k$
Correction step:
$\mathbf{H}_k = \frac{\partial \mathbf{f_d}}{\partial \mathbf{x}_k^*}\Big\|_{\mathbf{x}_k^*=\hat{\mathbf{x}}_k^{*-}}$
$\mathbf{G}_k = \mathbf{P}_k^- \mathbf{H}_k^T (\mathbf{H}_k \mathbf{P}_k^- \mathbf{H}_k^T + \mathbf{R}_k)^{-1}$
$\hat{\mathbf{x}}_k^{*+} = \hat{\mathbf{x}}_k^{*-} + \mathbf{G}_k(\mathbf{y}_k - \mathbf{H}\hat{\mathbf{x}}_k^{*-})$
$\mathbf{P}_k^+ = (\mathbf{I} - \mathbf{G}_k \mathbf{H}_k)\mathbf{P}_k^-$

3 Virtual sensing for contact parameter estimation

This section described the overall Virtual Sensing for contact parameter estimation and explains how the AEKF framework introduced in Section 2 is modified in order to handle issues posed by the estimation of contact parameters. Section 3.1 describes the lumped-parameter model used within the AEKF. Observability of the augmented states for the case of contact parameter estimation is discussed in Section 3.2. Section 3.3 describes how inequality constraints can be used to robustify the estimation process by avoiding physically inconsistent parameter estimates.

3.1 System under investigation

In order to better introduce the methodology developed in this section, a reference lumped-parameter model is adopted. This model is also used to perform the numerical experiments in Section 4. A representation is shown in Figure 2. Each of the four rigid spherical bodies can translate along the q_1, q_2, q_3, q_4 directions.

- Bodies 1 and 4 are connected with springs and dampers to the ground.
- Bodies 1-2 and 3-4 are also connected with springs and dampers.
- Bodies 2-3 can enter into contact, where a contact model represents this interaction.

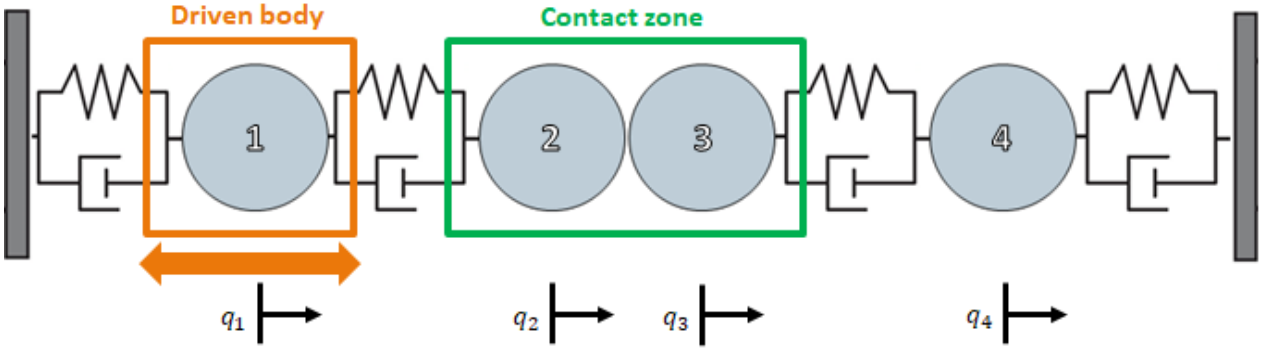

Figure 2: Lumped-parameter model. Bodies 1 and 4 are connected to the ground and to bodies 2 and 3 via springs and dampers. Bodies 2-3 interact via a contact model.

Body 1 moves under the influence of a known oscillating input force. The motion of body 1 forces bodies 2 and 3 to enter into and exit contact multiple times. The contact interaction between bodies 2 and 3 is modeled using a Hertzian contact formulation [11]:

$$f_c = \gamma(\text{ geometry, material })\delta^{\frac{3}{2}} \tag{16}$$

Here, the contact force f_c is defined as a nonlinear function of the contact stiffness γ, which is a function of the geometry of the contacting surfaces and the materials of the contacting bodies, and of the contact penetration δ. For the considered case, the parameter γ is constant and positive. The contact penetration δ is calculated from the relative position of bodies 2-3, and its sign defines if the contact interaction is active or not. The contact force f_c is non-zero only when contact is active. In the context of this paper, the following convention is therefore used:

$$\begin{cases} \delta > 0 & \text{Contact active, } f_c > 0 \\ \delta < 0 & \text{Contact not active, } f_c = 0 \end{cases} \tag{17}$$

Omitting ω_k, ϵ_k from notation for brevity, the discrete-time state-space formulation for the reference lumped-parameter model can be stated as:

$$\mathbf{x}^* = \begin{bmatrix} \mathbf{x} \\ \mathbf{p} \end{bmatrix} = \begin{bmatrix} \mathbf{q} \\ \mathbf{v} \\ \mathbf{p} \end{bmatrix} \tag{18}$$

$$\begin{cases} \frac{1}{\Delta t}(\mathbf{q}_k - \mathbf{q}_{k-1}) - \mathbf{v}_k = \mathbf{0} \\ \frac{1}{\Delta t}\mathbf{M}(\mathbf{v}_k - \mathbf{v}_{k-1}) + \mathbf{K}\mathbf{q}_k - \mathbf{B_u}\mathbf{u}_k - \mathbf{B_c}f_c(\mathbf{q}_k, \mathbf{p}_k) = \mathbf{0} \\ \mathbf{p}_k - \mathbf{p}_{k-1} = \mathbf{0} \\ \mathbf{y}_k = \mathbf{h}(\mathbf{q}_k, \mathbf{v}_k, \mathbf{p}_k) \end{cases} \tag{19}$$

Here, $\mathbf{q} \in \mathbb{R}^{n_q}$ is the coordinate vector, $\mathbf{v} \in \mathbb{R}^{n_v = n_q}$ is the velocity vector, $\mathbf{M} \in \mathbb{R}^{n_q \times n_q}$ is the mass matrix, $\mathbf{K} \in \mathbb{R}^{n_q \times n_q}$ is the stiffness matrix, $\mathbf{B_u} \in \mathbb{R}^{n_q \times n_i}$ is the input distribution matrix, $\mathbf{B_c}(\mathbf{q}, \mathbf{p}) \in \mathbb{R}^{n_q} \times 1$ is the contact force distribution matrix, Δt is the timestep size. It is assumed that $\mathbf{M}, \mathbf{K}, \mathbf{B_u}, \mathbf{B_c}$ are constant and that the only source of non-smoothness and nonlinearity is $\mathbf{f_c}$, which is the only term that depends on $\mathbf{p}$.

In this work, $\mathbf{p} = \gamma$ (and thus $n_p = 1$). Given the fact that γ is only affecting the motion of the system during contact, the corresponding impact on the system observability is further considered below.

3.2 Observability analysis

The system observability is a key property for the AEKF as it determines whether a state can be estimated and the estimator remains stable. The observability depends on the combination of model equations and measurement equations. The issue of observability of inputs and parameters in Virtual Sensing has been widely explored in multiple works [3, 5, 12]. In order to have a stable estimator for the Virtual Sensing application developed in this work, a sufficient condition is that the system in Eq. (7) is locally observable. In this work, the Popov-Belevitch-Hautus (PBH) test for observability is applied on the linearized continuous-time system for the evaluation of local observability [13]. The criterion states that the system is observable if and only if the matrix in Eq. (20) is of full rank for all $s \in \mathbb{C}$.

$$\mathcal{O}_{\text{PBH}}(s) = \begin{bmatrix} \mathbf{A} - s\mathbf{I} \\ \mathbf{H} \end{bmatrix} \tag{20}$$

Here, $\mathbf{A}$ is the continuous time Jacobian of the augmented system described in Eq. (3) and is obtained by following the continuous-time equivalent of the procedure described in Eq. (10), while $\mathbf{H}$ is obtained by linearizing Eq. (5). In order to perform this test, it is sufficient to check the rank of $\mathcal{O}$ at the eigenvalues λ of $\mathbf{A}$. Considering the lumped-parameter system introduced in Section 3.1, it possible to distinguish between two different system configurations, based upon the contact being active or not. The following considerations are made:

- If contact is active, the system is locally observable if the number of independent position-level measurements (e.g., position or strain measurements) is equal or greater than the number of parameters to be estimated, i.e. $n_o(\text{pos. level meas.}) \geq n_p$. In this case, a single position-level measurement is sufficient for local observability [3, 5].
- If contact is inactive, the system is locally unobservable. This conclusion can also be reached via physical intuition, as the contact parameter γ, part of the augmented state of the system, does not influence the dynamics of the system in this configuration.

In order to ensure the stability of the estimator in the unobservable configuration, a switch-off approach similar to the ones developed in [9] and [8] is adopted. With reference to Eq. (8), the term $\mathbf{Q_p} = Q_\gamma$ is defined differently according to the system configuration:

$$\begin{cases} \delta_k > 0 & \text{Contact active, } Q_\gamma \neq 0 \\ \delta_k < 0 & \text{Contact not active, } Q_\gamma = 0 \end{cases} \tag{21}$$

The propagation of the state error covariance matrix $\mathbf{P}$ is different according to active system configuration. The substructure of $\mathbf{P}$ is specified as follows:

$$\mathbf{P} = \begin{bmatrix} \mathbf{P_{xx}} & \mathbf{P_{x\gamma}} \\ \mathbf{P}_{\mathbf{x}\gamma}^T & P_{\gamma\gamma} \end{bmatrix} \tag{22}$$

Propagation of the covariance terms related to γ (the submatrices $\mathbf{P_{x\gamma}}$ and $\mathbf{P}_{\gamma\gamma}$) is prevented by keeping these terms constant when contact is not active. In the same fashion, the estimate $\hat{\gamma}$ is not allowed to vary when contact is not active.

When contact is active during the time update step, only $\mathbf{P_{xx}}$ is propagated as follows:

$$\mathbf{F}_k = \begin{bmatrix} \mathbf{F}_{\mathbf{xx},k} & \mathbf{F}_{\mathbf{x}\gamma,k} \\ \mathbf{0} & 1 \end{bmatrix} \tag{23}$$

$$\mathbf{P}_{\mathbf{xx},k}^- = \mathbf{F}_{\mathbf{xx},k}\mathbf{P}_{\mathbf{xx},k-1}^+\mathbf{F}_{\mathbf{xx},k}^T + \mathbf{Q}_{\mathbf{x},k} \tag{24}$$

Similarly, when contact is active during the correction step:

$$\mathbf{H}_k = \begin{bmatrix} \mathbf{H}_{\mathbf{x},k} & \mathbf{H}_{\gamma,k} \end{bmatrix} \tag{25}$$

$$\mathbf{G}_k = \begin{bmatrix} \mathbf{G}_{\mathbf{x},k} \\ \mathbf{G}_{\gamma,k} \end{bmatrix} \tag{26}$$

$$\mathbf{P}^+_{\mathbf{xx},k} = (\mathbf{I} - \mathbf{G}_{\mathbf{x},k}\mathbf{H}_{\mathbf{x},k})\mathbf{P}^-_{\mathbf{xx},k} \tag{27}$$

3.3 Inequality constraints

The Kalman filter formulation can be extended to enforce linear inequality constraints on the augmented state $\mathbf{x}^*$ during the estimation process [6, 7]. Considering a single inequality constraint c, this can be expressed as:

$$c = \mathbf{D}\mathbf{x}^* - d \geq 0 \tag{28}$$

Where $\mathbf{D}$ and d represent the linear constraint matrix of the system state $\mathbf{x}^*$ and the constraint value, respectively. During each time step, the constraint equation c is evaluated after the correction step. If c is violated, the correction step is repeated using an augmented measurement equation (i.e. a perfect measurement approach).

$$\mathbf{y}^{\mathbf{c}}_{\mathbf{k}} = \begin{bmatrix} \mathbf{y}_{\mathbf{k}} \\ d \end{bmatrix} = \begin{bmatrix} \mathbf{H} \\ \mathbf{D} \end{bmatrix} \mathbf{x}^*_k + \begin{bmatrix} \epsilon_k \\ 0 \end{bmatrix} = \mathbf{H}^c \mathbf{x}^*_k + \epsilon^c_k \tag{29}$$

$$\mathbf{R}^{\mathbf{c}} = \begin{bmatrix} \mathbf{R} & \mathbf{0} \\ \mathbf{0} & \mathbf{0} \end{bmatrix} \tag{30}$$

The Kalman gain $\mathbf{G}$ is recomputed from Eq. (13) using $\mathbf{H}^{\mathbf{c}}$ and $\mathbf{R}^{\mathbf{c}}$ instead of $\mathbf{H}$ and $\mathbf{R}$ to enforce the violated inequality constraint. Using inequality constraints robustifies the estimation process, especially when dealing with parameter estimation, as it restricts the filter from estimating physically inconsistent or inadmissible parameter values. When estimating γ, inequality constraints can prevent the filter from estimating a negative value for the contact stiffness.

4 Numerical validation

This section demonstrates the potential of the methodology developed in Section 3 by means of a numerical estimation exercise. The model described in Section 3 is used. The translation of body 1 is controlled using a driver which imposes a low-frequency (0.05 Hz) sinusoidal motion. This in turn excites the entire system via the spring-damper elements and the contact interaction. A Newton-Rhapson scheme is used within the AEKF to solve the nonlinear equations of motion (Eq. (7)).

Virtual measurement data is generated by means of a forward simulation using the reference model. This virtual measurement data is used to perform the joint estimation of the system state $\mathbf{x}$ and the contact stiffness parameter γ. It is assumed that no noise is present on the generated measurements. Position measurements of bodies 1 and 4 are used by the AEKF. This fulfills the observability requirements when contact is active, as described in Section 3.2. Regarding the process noise covariance matrix $\mathbf{Q}$, it is assumed that most of the model uncertainty is on the contact parameter γ, such that $Q_\gamma \gg Q_{\mathbf{x},j}$ for all the j diagonal terms of $\mathbf{Q}_{\mathbf{x}}$. This is justified by the fact that the estimator assumes an initial value for $\hat{\gamma}$ that is 25% lower than the correct reference value. The objective of the estimator is to correct this value and, as a consequence, yield an overall better estimate of the system state.

4.1 Benchmarking the AEKF for contact parameter estimation

In order to assess the performance of the developed AEKF formulation for contact parameter estimation, a comparison with the canonical AEKF formulation is considered. The setup of both of these estimators is exactly the same, but the AEKF for contact includes the proposed switch-off methodology described in Section 3.2.

A useful indicator for tracking the stability of the estimator is the norm of $\mathbf{P}$ throughout the estimation process. A comparison of $||\mathbf{P}||$ is presented in Figure 3. Due to unobservability of the system, $||\mathbf{P}||$ for the canonical AEKF formulation does not converge to a stable pattern, while it does for the developed AEKF for contact, indicating a stable estimate has been obtained.

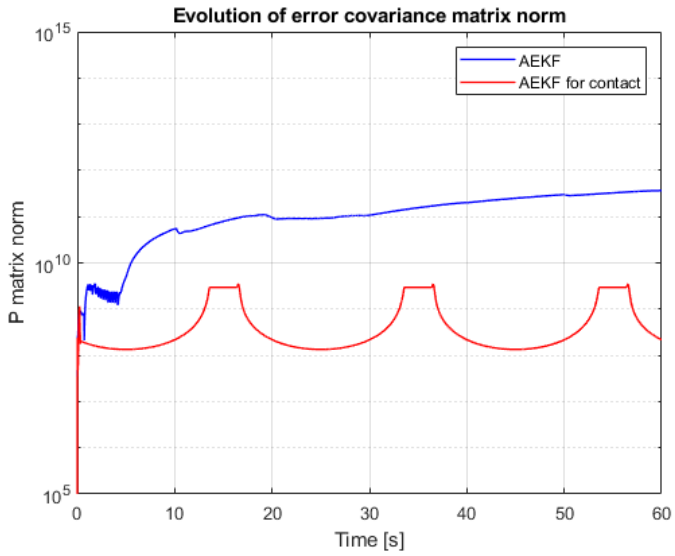

Figure 3: Comparison of the error covariance matrix $\mathbf{P}$ norm evolution during the estimation process between a standard AEKF and the AEKF for contact parameter estimation. The continuously growing norm for the AEKF (blue curve) implies that the estimator is not stable.

The effect of unobservability is also visible in the state and parameter estimates. Figure 4 shows the estimate of γ. The canonical AEKF estimate is unstable, while the AEKF for contact is stable and capable of estimating the parameter. The γ estimate affects the accuracy of state estimates. Figure 5 shows the estimate of body 2's position for both estimators. The AEKF estimate is generally less accurate than the AEKF for contact, as a consequence of the instability of the γ estimate for the first estimator. This inaccuracy increases near a contact event, which in this case happens in the 14-15s time range. The AEKF for contact is capable of producing an overall more accurate estimate of states and parameters.

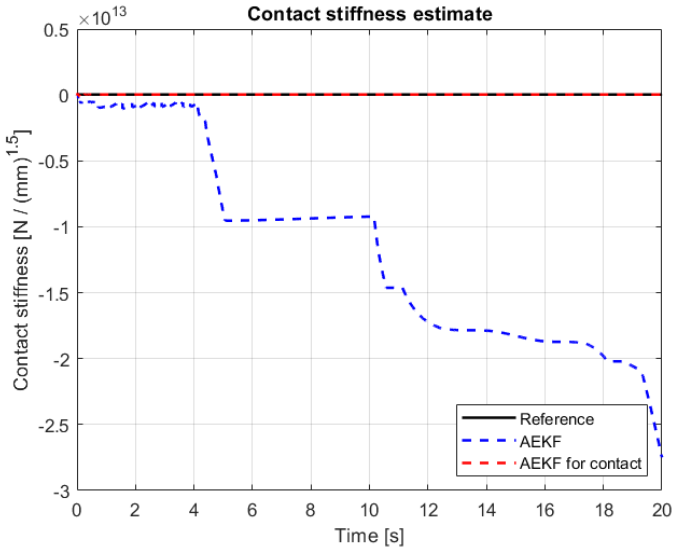

Figure 4: Estimate of contact stiffness, comparison between the AEKF (blue) and the AEKF for contact (red). The reference stiffness value is shown as the black curve. The AEKF does not reach a stable estimate due to not being able to handle the system unobservability.

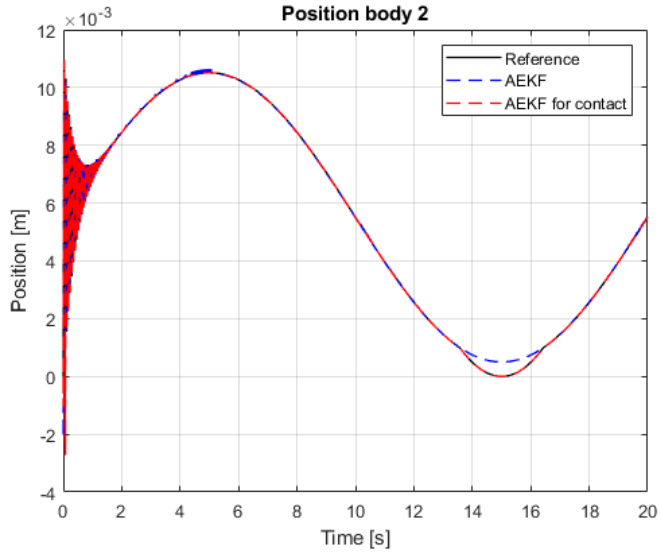

Figure 5: Position estimate for body 2, comparison between the AEKF (blue) and the AEKF for contact (red). The reference position is shown as the black curve.

4.2 Including inequality constraints

While the AEKF for contact is more stable than the canonical AEKF, its estimates can still be compromised if the value of Q_γ is not correctly set up. An exceedingly high level of process noise can lead to excessive oscillations in the parameter estimate, which presents the risk of obtaining physically inconsistent estimates, such as a negative γ value, similarly to what is obtained in Figure 4 for the standard AEKF. Correctly tuning Q_γ can be a time-consuming process and is often done by trial and error.

Including inequality constraints into the estimation process, following the procedure introduced in Section 3.3, allows to enforce the value of γ to be in a specified range and to mitigate the issue described above.

The effect of including these inequality constraints is shown in Figure 6. These estimation results are obtained with a value of Q_γ that is 3 orders of magnitude the one used for Section 4.1. Due to the large value of Q_γ, the *unconstrained* AEKF for contact obtains negative contact stiffness estimates, which compromises the overall estimation accuracy. The *constrained* AEKF for contact, which incorporates inequality constraints that enforce γ to be positive, is however capable of obtaining a stable contact stiffness estimate.

The usage of inequality constraints therefore robustifies the estimation procedure and can be integrated into the estimation process, using straightforward physical reasoning for the choice of constraints to be enforced.

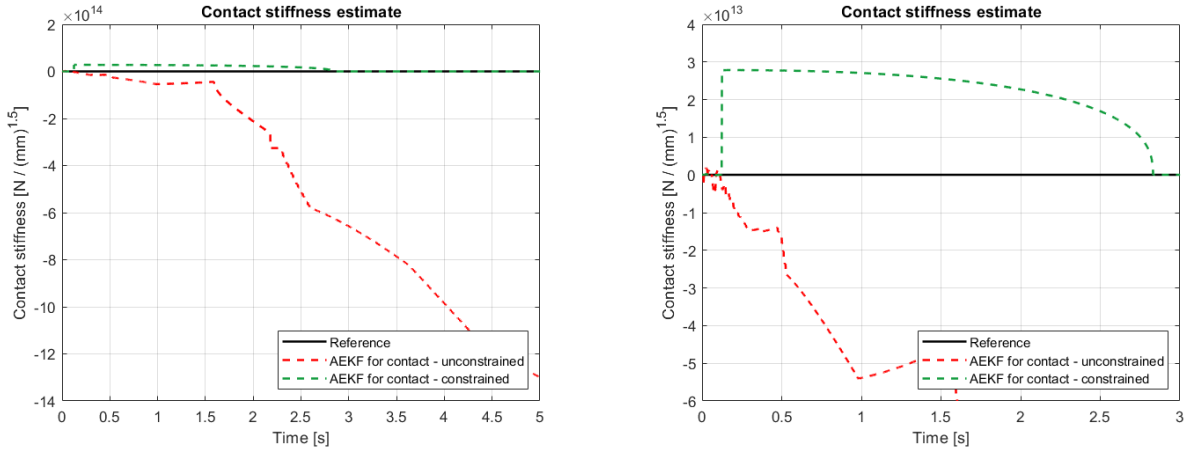

(a) Parameter estimate with AEKF for contact: unconstrained vs. constrained.

(b) Detail of parameter estimate with AEKF for contact: unconstrained vs. constrained.

Figure 6: Estimate of the contact stiffness, comparison between the unconstrained AEKF for contact (red) and the constrained AEKF for contact (green). The reference stiffness value is shown as the black curve. The unconstrained AEKF for contact does not reach a stable estimate as it allows the contact stiffness estimate to become negative.

5 Conclusions

In this paper, a Virtual Sensing framework for contact model parameter estimation is presented. Starting from an Augmented Extended Kalman filter approach, the estimation framework has been adapted to contact mechanics, which is mainly characterized by the non-smoothness and nonlinearity of the contact interactions. The issue of system unobservability when contact model parameters are used as augmented states has been addressed by means of a switch-off strategy. Additionally, a perfect measurement approach has been included to enforce inequality constraints and physically consistent parameter value estimates. The potential of the developed methodology has been shown using a numerical example. A lumped-parameter model consisting of four bodies connected with springs, dampers and a Hertzian contact interaction between two of the bodies has been used to generate simulated, virtual position-level measurements. These measurements, together with the lumped-parameter model, have been used to successfully estimate the contact stiffness parameter of the Hertzian contact model using the proposed Virtual Sensing framework, showcasing the overall quality and robustness of the methodology.

Acknowledgements

The authors gratefully acknowledge the support and contribution of the European Commission with Marie Sklodowska Curie program through the ETN ECO DRIVE project n. GA 858018. This research was partially supported by VLAIO (Flanders Innovation & Entrepreneurship Agency) within the O&O project IMPROVED (effIcient Model-based oPeRatiOnal VEhicle Dynamics testing).

References

[1] P. Wriggers, *Computational contact mechanics*, 2012, vol. 49.

[2] E. Lourens, E. Reynders, G. D. Roeck, G. Degrande, and G. Lombaert, "An augmented kalman filter for force identification in structural dynamics," *Mechanical Systems and Signal Processing*, vol. 27, 2012.

[3] F. Naets, J. Cuadrado, and W. Desmet, "Stable force identification in structural dynamics using kalman filtering and dummy-measurements," *Mechanical Systems and Signal Processing*, vol. 50-51, 2015.

[4] E. Risaliti, T. Tamarozzi, M. Vermaut, B. Cornelis, and W. Desmet, "Multibody model based estimation of multiple loads and strain field on a vehicle suspension system," *Mechanical Systems and Signal Processing*, vol. 123, pp. 1–25, 5 2019.

[5] R. Cumbo, L. Mazzanti, T. Tamarozzi, P. Jiranek, W. Desmet, and F. Naets, "Advanced optimal sensor placement for kalman-based multiple-input estimation," *Mechanical Systems and Signal Processing*, vol. 160, p. 107830, 11 2021.

[6] D. Simon, *Optimal state estimation: Kalman, H∞, and nonlinear approaches*, 2006.

[7] B. O. S. Teixeira, J. Chandrasekar, L. A. B. Tôrres, L. A. Aguirre, and D. S. Bernstein, "State estimation for linear and non-linear equality-constrained systems," *International Journal of Control*, vol. 82, pp. 918–936, 2009. [Online]. Available: https://doi.org/10.1080/00207170802370033

[8] M. N. Chatzis, E. N. Chatzi, and S. P. Triantafyllou, "A discontinuous extended kalman filter for non-smooth dynamic problems," *Mechanical Systems and Signal Processing*, vol. 92, 2017.

[9] F. Naets, S. van Aalst, B. Boulkroune, N. E. Ghouti, and W. Desmet, "Design and experimental validation of a stable two-stage estimator for automotive sideslip angle and tire parameters," *IEEE Transactions on Vehicular Technology*, vol. 66, pp. 9727–9742, 11 2017.

[10] R. Cumbo, T. Tamarozzi, K. Janssens, and W. Desmet, "Kalman-based load identification and full-field estimation analysis on industrial test case," *Mechanical Systems and Signal Processing*, vol. 117, pp. 771–785, 2019. [Online]. Available: https://www.sciencedirect.com/science/article/pii/S0888327018305818

[11] R. G. Ali M. Sadegh Budynas, "Roark's formulas for stress and strain, ninth edition," *Studies in Applied Mechanics*, vol. 4, 1980.

[12] T. Tamarozzi, E. Risaliti, W. Rottiers, K. janssens, and W. Desmet, "Noise, ill-conditioning and sensor placement analysis for force estimation through virtual sensing." Katholieke Univ. Leuven, Dept. Werktuigkunde, 2016, pp. 1741–1756.

[13] B. Ghosh and J. Rosenthal, "A generalized popov-belevitch-hautus test of observability," *IEEE Transactions on Automatic Control*, vol. 40, no. 1, pp. 176–180, 1995.